

Shape fluctuations and elastic properties of two-component bilayer membranes

ALBERTO IMPARATO¹ (*), JULIAN C. SHILLCOCK¹ and REINHARD LIPOWSKY¹

¹ *Max-Planck-Institut für Kolloid- und Grenzflächenforschung,
14424 Potsdam, Germany.*

PACS. 87.16.Dg – Membranes, bilayers, and vesicles.

PACS. 82.70.-y – Disperse systems, complex fluids.

PACS. 61.20.Ja – Computer simulation of liquid structure.

Abstract. – The elastic properties of two-component bilayer membranes are studied using a coarse grain model for amphiphilic molecules. The two species of amphiphiles considered here differ only in their length. Molecular Dynamics simulations are performed in order to analyze the shape fluctuations of the two-component bilayer membranes and to determine their bending rigidity. Both the bending rigidity and its inverse are found to be nonmonotonic functions of the mole fraction x_B of the shorter B-amphiphiles and, thus, do not satisfy a simple lever rule. The intrinsic area of the bilayer also exhibits a nonmonotonic dependence on x_B and a maximum close to $x_B \simeq 1/2$.

Biological membranes are multicomponent systems consisting of mixtures of many different lipids and proteins. Because the composition of lipid bilayers affects their physical properties and biological functions, this composition varies from one organism to the other and between organelles in the same cell [1]. Biological membranes contain a fluid bilayer which is highly flexible and, thus, can easily change its shape. Typical examples are provided by the plasma membranes of red and white blood cells which are so flexible that they can move through rather small capillaries. This flexibility is also responsible for the thermally excited shape fluctuations of biomembranes in physiological conditions, the amplitude of which depends on temperature, membrane composition and mechanical constraints. One important example is provided by mixed membranes containing phospholipids and cholesterol which exhibit a strong increase in rigidity with increasing amount of cholesterol [2–4]. In erythrocytes, on the other hand, the amplitude of the shape fluctuations is influenced by the spectrin-ankyrin network which is coupled to the interior of the plasma membrane [5,6]. The study of these fluctuations can thus provide information on the elastic properties of the bilayer membrane and on how these properties depend on membrane composition. One important elastic parameter is the *bending rigidity* [7], which describes the resistance of the membrane to bending, and which can be obtained from the spectrum of the shape fluctuations [8].

(*) Present address: Dipartimento di Scienze Fisiche and Unità INFN, Università “Federico II”, Complesso Universitario di Monte S. Angelo, I-80126 Napoli (Italy).

In spite of their complex chemical composition, all biomembranes have the same basic structure: a bilayer of lipid and protein molecules. Therefore the simplest model for a biological membrane is a bilayer of amphiphilic molecules as studied in the present work. The bending rigidity of such bilayers has already been determined via computer simulations both for coarse grain models of amphiphile-water systems [9,10] and for models with atomic resolution [11]. In all of these previous studies, the bilayers contained only a single component in contrast to natural membranes which contain many different types of lipids and proteins.

In the present article, we study bilayer membranes with two components and determine the dependence of their elastic properties on membrane composition. We use a coarse grain model for the amphiphiles and for the water particles which we investigate by Molecular Dynamics simulations. The two species of amphiphiles considered here differ only in their length. This choice allows us to focus on the contribution from the mismatch of the amphiphile tails.

Two types of theories have previously addressed the bending elasticity of two-component bilayers. First, a self-consistent (or molecular field) theory was used to estimate the contribution to the bending rigidity arising from the conformations of the amphiphilic tails [12]. Secondly, the so-called hat model for local curvature fluctuations was used in order to derive an expression for the bending rigidity of two-component bilayers [13]. The predictions of these two theories are different as far as the functional dependence of bending rigidity on composition is concerned. On the one hand, the results of the self-consistent theory for the chain conformations depend on the types of packing constraint acting on the conformations of a single tail. The hat model, on the other hand, predicts that the inverse bending rigidity (or flexibility) satisfies a simple ‘lever rule’ corresponding to a linear interpolation between the two limiting values for the one-component bilayers.

In contrast to the analytical but approximate theories in [12] and [13], our simulations take all types of fluctuations into account: different tail conformations; curvature (or bending) fluctuations; molecular protrusions; and composition fluctuations arising from lateral diffusion. We find that both the bending rigidity and its inverse exhibit a nonmonotonous behavior as a function of the mole fraction x_B . Our results are qualitatively similar to the self-consistent theory, *provided* one uses the packing constraint of ‘constant area’ per molecule, but show that a simple lever rule for the inverse bending rigidity does not apply in general.

The coarse grain model used here consists of several types of particles: water particles, which correspond to several water molecules, as well as head group and tail particles, which represent the head groups and the hydrocarbon tails of the amphiphilic molecules, respectively. The two species of amphiphiles will be denoted by A and B. Both types of amphiphiles are composed of one head group particle, which is hydrophilic, and of several tail particles, which are hydrophobic. The different length of the two molecular species arises from the different number of tail particles which is four and two for A and B, respectively, see figure 1. The

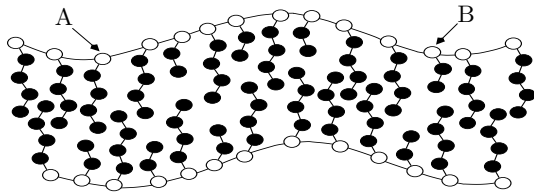


Figure 1 – Cartoon of a two-component bilayer.

particles experience attractive and repulsive pair-interactions which are modelled by Lennard-Jones (LJ) and Soft-Core potential (SC), respectively. The parametrization of these potentials

has been previously described in [14] where the same model was used in order to study the lateral and transverse diffusion within the two-component bilayer membranes. Within this model, all quantities can be expressed in terms of three basic scales: the particles mass m , the LJ interaction energy ϵ and the LJ radius ρ . As in [14] and [15], we chose the numerical values $mN_{Av} = 3.6 \cdot 10^{-2}\text{kg}$, $\epsilon N_{Av} = 2\text{kJ}$, and $\rho = 1/3 \text{ nm}$, where N_{Av} is the Avogadro number. Our MD simulations are carried out for a cuboidal box of constant volume and periodic boundary conditions using a constant temperature algorithm with $k_B T = 1.35\epsilon$. The starting configurations for the two-component bilayer simulations are such that each monolayer contains the same number of A and B molecules. We checked that, in each monolayer, the average number of B molecules did not change during the simulations. While multicomponent bilayer membranes may exhibit deviations from ideal mixing behavior [16] and may, in general, undergo phase separation, the two-component bilayers studied here stayed in the one-phase region over the whole range $0 \leq x_B \leq 1$ of mole fractions for the B molecules. Thus, our bilayers correspond to a lipid mixture above the liquidus–solidus line.

The elastic properties of a fluid membrane which has vanishing spontaneous curvature are governed by its bending rigidity κ and by its surface tension σ . These quantities can be determined from the spectrum of the shape fluctuations. In order to do so, we choose the (x, y) -plane to be parallel to the bilayer membrane. The shape of the membrane is then described by the height function $h(x, y)$ which measures the distance of its midsurface from the (x, y) -plane. We define the Fourier coefficients $\tilde{h}_{\mathbf{q}} \equiv A_p^{-1} \int_{A_p} dx dy \exp[-i(xq_x + yq_y)] h(x, y)$, with $\mathbf{q} \equiv (q_x, q_y)$, where A_p is the projected area of the membrane. Its fluctuation spectrum, $S(q) \equiv \langle |\tilde{h}_{\mathbf{q}}|^2 \rangle$, depends only on $q = |\mathbf{q}|$ and exhibits the functional form

$$S(q) = k_B T / [A_p (\sigma q^2 + \kappa q^4)] \quad (1)$$

for long-wavelength bending modes [8], and the somewhat different form

$$S(q) = k_B T / (A_p \sigma_{pr} q^2) \quad (2)$$

for short-wavelength molecular protrusions [17]. Apart from the temperature T and the projected area A_p , the two spectra as given by (1) and (2) contain three parameters: the surface tension σ , the bending rigidity κ , and the protrusion tension σ_{pr} . As discussed in [15], the lateral size of the simulation box can be adjusted in order to obtain a bilayer with vanishing thermodynamic tension. This latter procedure consists in determining, for fixed particle number, fixed volume, and fixed temperature, the stress (or pressure) tensor which has a tangential component, Σ_T , and a normal component, Σ_N [15]. Both components depend on the coordinate z perpendicular to the membrane. The thermodynamic tension Σ is then obtained from $\Sigma = \int dz [\Sigma_T(z) - \Sigma_N(z)]$. It is intuitively appealing to identify the thermodynamic tension Σ with the surface tension σ which governs the fluctuation spectrum. Indeed, this assumption was implicit in our previous work in [9] and was found to be satisfied within the accuracy of the simulation data obtained there. However, more extensive simulations have shown that this identity does not hold in general [18]. This difference is related to the fact that Σ is conjugate to the projected area, whereas σ is conjugate to the intrinsic area, a distinction which has been previously discussed, e.g., in [19]. Therefore, in the present work, we used an improved procedure in order to determine the state with $\sigma = 0$: for fixed particle number and fixed temperature, we adjusted the lateral box size in order to obtain a fluctuation spectrum $S(q)$ which can be well fitted, for small q , by the form (1) with $\sigma = 0$ [18].

First, let us discuss this fitting procedure for one-component bilayers corresponding to vanishing mole fraction $x_B = 0$. An example of the measured fluctuation spectrum $S(q)$ for $N_A = 1152$. is shown in figure 2. The lines, which represent the functional forms as given by

(1) with $\sigma = 0$ and by (2), respectively, are plotted in the same figure. From these fits, we obtain the values $\kappa = 3.0 \pm 0.2 k_B T$ and $\sigma_{pr} = 2.50 \pm 0.03 \epsilon/\rho^2$. Essentially the same values are found for $N_A = 512$: $\kappa = 3.20 \pm 0.06 k_B T$ and $\sigma_{pr} = 2.65 \pm 0.05 \epsilon/\rho^2$ [18]. For surface

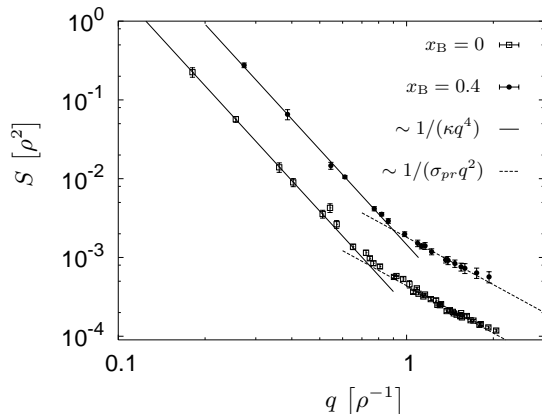


Figure 2 – Fluctuation spectrum S for one and two-component bilayers with $N_A = 1152$ ($x_B = 0$) and $N = 512$ ($x_B = 0.4$), respectively, in tension-free state. The lines are obtained by fitting the fluctuation spectra of the tensionless systems, using eq. (1) (full lines) and eq. (2) (dashed lines) at small and large q , respectively. The units are given in brackets.

tension $\sigma = 0$, the intrinsic area per molecule, a_{in} , is expected to attain a certain value which is determined by the optimal packing of the molecules within the bilayer and, thus, should not depend on the overall size of the membrane. Indeed, if we adjust the box size to obtain vanishing surface tension $\sigma \simeq 0$, our MD simulations lead to $a_{in} = 2.26 \pm 0.01 \rho^2$ for $N_A = 512$ and to $a_{in} = 2.277 \pm 0.005 \rho^2$ for $N_A = 1152$ which are identical within the numerical accuracy.

Next, we consider two-component bilayers with mole fraction $0 < x_B < 1$. To save computation time, we varied the mole fraction x_B for fixed total number $N = N_A + N_B$ of the amphiphiles with $N = 512$. In order to attain tensionless states of the two-component bilayers, the projected area A_p has to be gradually decreased as x_B is increased, since the projected area per molecule, $a_p \equiv 2A_p/N$, is smaller for the B-amphiphile than for the A-amphiphile. The measured fluctuation spectrum $S(q)$ for $x_B = 0.4$ is also shown in figure 2.

In figure 3(a), the bending rigidity κ is plotted as a function of x_B . For the pure A-bilayer and the pure B-bilayer, we find $\kappa_A = 3.20 \pm 0.06 k_B T$ and $\kappa_B = 1.3 \pm 0.1 k_B T$, respectively. As shown in figure 3(a), the bending rigidity is nonmonotonic for intermediate values of x_B and exhibits a minimum for $x_B \simeq 0.6$ with $\kappa = 1.0 \pm 0.1 k_B T$. Figure 3(b) displays the inverse bending rigidity $1/\kappa$ as a function of the mole fraction x_B . For this latter quantity, a simple lever rule as given by $1/\kappa = x_B/\kappa_B + (1 - x_B)/\kappa_A$ has been proposed in [13]. Inspection of figure 3(b) shows that such a lever rule does not apply here. However, our data are consistent with the more general proposal that the bending rigidity behaves smoothly both at $x_B = 0$ and at $x_B = 1$. Indeed, we conclude from the data in figure 3(b) that

$$1/\kappa \approx (1/\kappa_A)(1 + \phi_{AB}x_B) \quad \text{with} \quad \phi_{AB} = 3.5 \pm 0.1 \quad (3)$$

for small x_B and that

$$1/\kappa \approx (1/\kappa_B)(1 + \phi_{BA}x_A) \quad \text{with} \quad \phi_{BA} = 1.0 \pm 0.2 \quad (4)$$

for small $x_A = 1 - x_B$.

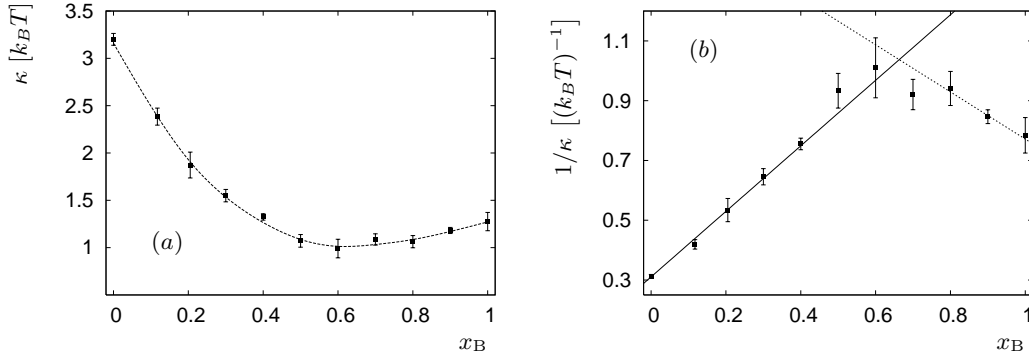


Figure 3 – (a) Bending rigidity κ and (b) inverse bending rigidity of two-component A- B-bilayers vs. the shorter amphiphile mole concentration x_B . The error bars represent statistical errors obtained by the fit of the fluctuation spectrum data to eq. (1). In (a) the line is obtained by fitting the data with a smoothing spline. In (b) the full and dotted line correspond to linear fit to the data for $x_B \leq 0.4$ and $x_B \geq 0.8$, respectively. The units are given in brackets.

We also measured the intrinsic bilayer area A , defined by $A = \int_{A_p} dx dy \sqrt{1 + (\nabla h)^2}$. In Fig. 4, the intrinsic area per amphiphile, $a_{in} = 2A/N$, is plotted as a function of x_B for tensionless bilayer states. As shown in this figure, the intrinsic molecular area a_{in} is again found to be a nonmonotonic function of x_B : for $x_B = 0$, it has the value $a_{in} \simeq 2.26\rho^2$, but exhibits a maximum at $x_B = 0.4$ with $a_{in} \simeq 2.39\rho^2$. The change in the intrinsic area is obviously con-

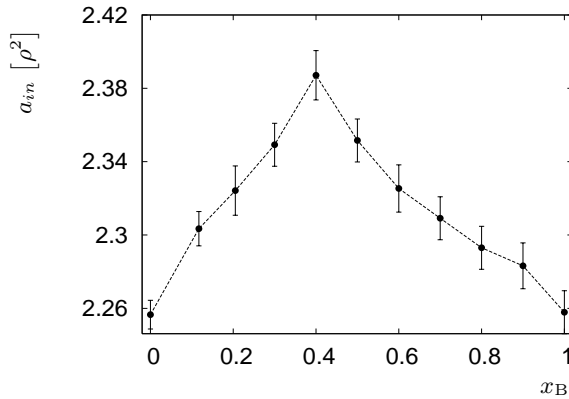


Figure 4 – Area per amphiphile $a_{in} = 2A/N$ vs. the shorter amphiphile mole concentration x_B . The error bars represent standard errors obtained from the area fluctuations. The line is a guide to the eye. The units are given in brackets.

nected to the change in the bending rigidity. The decrease of the latter quantity corresponds to a more flexible bilayer with larger shape fluctuations and a corresponding increase in the intrinsic area. Inspection of figure 4 shows that the pure A-bilayer has essentially the same intrinsic molecular area as the pure B-bilayer, i.e., $a_{in}(x_B = 0) \simeq a_{in}(x_B = 1) \simeq 2.26\rho^2$. In contrast, the corresponding *projected* molecular areas a_p are found to be $a_p(x_B = 0) = 2.10\rho^2$ and $a_p(x_B = 1) = 1.96\rho^2$ which reflects the increased shape fluctuations for $x_B = 1$.

Finally, the protrusion tension σ_{pr} as introduced in (2) also exhibits a nonmonotonic behavior as shown in Fig. 5. A decrease in the protrusion tension implies an increase in the amplitude of the local protrusions which become energetically more favorable. As shown in Fig. 5, σ_{pr} decreases with increasing x_B up to $x_B = 0.2$, then stays essentially constant up to $x_B = 0.8$, and finally increases again up to $x_B = 1$. This indicates that a small amount of shorter B–amphiphiles is sufficient to roughen the bilayer surface, and further addition of these amphiphiles has essentially no effect on the local protrusions until one reaches another regime characterized by a bilayer of B–amphiphiles with a few longer A–amphiphiles. Comparing the results for bending rigidity, intrinsic area and protrusion tension, one concludes that the changes in the intrinsic area depend both on the shape fluctuations and on the bilayer roughness arising from the local mismatch between the two types of amphiphiles.

The bending rigidity of amphiphilic bilayers has been measured in many experiments: while phospholipid membranes [4, 8, 20–22] are characterized by a bending rigidity of the order of tens of $k_B T$, lamellar and fluid microemulsion phases composed of single chain surfactants, short chain alcohols, oil and water [23–26] exhibit a bending rigidity of the order of $k_B T$. The bilayer studied in our Molecular Dynamics simulations are composed of single–chain amphiphiles and have bending rigidities which are of the same order of magnitude as those studied in the second group of experiments. In Refs. [23–25], the response of lamellar systems to the insertion of shorter cosurfactants was studied experimentally. In these systems, the main surfactant was sodium dodecyl sulfate (SDS), which is a single chain surfactant, while the cosurfactants were alcohol molecules: it was found that the bending rigidity decreases as the fraction of shorter chain cosurfactant increases. In Ref. [25], short surfactant (pentanol) molecules were added to bilayers composed of two–chain amphiphiles (DMPC) and a decrease of the bending rigidity was observed. Two–component bilayer membranes were also studied

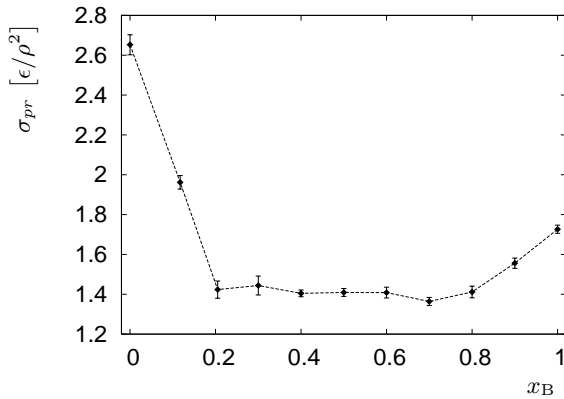


Figure 5 – Protrusion tension σ_{pr} vs. the shorter amphiphile mole concentration x_B . The error bars represent statistical errors obtained by the fit of the fluctuation spectrum data to eq. (2). The line is a guide to the eye. The units are given in brackets.

theoretically by Szleifer et al. [12] using a simple mean field theory to treat chain packing. In the framework of these theories, which are based on smooth bending configurations and, thus, neglect protrusions, the longer amphiphiles obtain more configurational freedom as the shorter amphiphiles are added which leads to an increased flexibility of the bilayers. The behavior of the bending rigidity as found in our simulations for small x_B is consistent with such a mechanism. However, we also find that both the bending rigidity and the protrusion

tension *decrease* as one adds long A–amphiphiles to a bilayer of short B–amphiphiles for large values of x_B , see Figs. 3 and 5. In this latter regime, the addition of the A–amphiphiles induces more protrusions which act to reduce the bending rigidity [17].

In conclusion, we have presented the results of Molecular Dynamics simulations for a coarse grain model of two-component bilayers. We show that the functional dependence of the inverse bending rigidity on the membrane composition does not follow a simple lever rule. In contrast, we find that both the addition of short amphiphiles to a bilayer of long ones and the addition of long amphiphiles to a bilayer of short ones leads to an increase in molecular protrusions and to a decrease in the bending rigidity. We also observe a nonmonotonic functional dependence of the intrinsic area on the membrane composition which is strongly correlated with the behavior of both local protrusions and long–wavelength shape fluctuations. The simulation approach described here can be extended to bilayer membranes with three components which have recently been shown to lead to coexisting membrane domains or ‘rafts’ and to more realistic models of biological membranes which contain membrane proteins.

References

- [1] R. Lipowsky and E. Sackmann, *The Structure and Dynamics of Membranes*, (Elsevier, Amsterdam 1995).
- [2] H. P. Duwe, J. Kaes, E. Sackmann *J. Phys. France* **51**:945-962 (1990).
- [3] E. Evans and W. Rawicz, *Phys. Rev. Lett.* **64**: 2094 (1990).
- [4] P. Meleard et al, *Biophys. J.* **72**:2616-2629 (1997).
- [5] R. Waugh and E.A. Evans, *Biophys. J.* **26**: 115-131 (1979).
- [6] H. Strey, M. Peterson and E. Sackmann, *Biophys. J.* **69**: 478-488 (1995).
- [7] P.B. Canham, *J. Theor. Biol* **26**:61-81 (1970); W. Helfrich, *Z. Naturforsch.*, **28c**:693 (1973).
- [8] J.F. Lennon and F. Brochard, *J. Phys. (Paris)* **36**: 1035 (1975).
- [9] R. Goetz, G. Gompper and R. Lipowsky *Phys. Rev. Lett.* **82**:221-224 (1999).
- [10] S.J. Marrink, A.H. de Vries and A.E. Mark, *J. Phys. Chem. B* **108**:750-760 (2004).
- [11] E. Lindahl and O. Edholm, *Biophys. J.* **79**:426-433 (2000); S.J. Marrink and A.E. Mark, *J. Phys. Chem.* **105**:6122-6127 (2001); J. C. Shelley et al, *J. Phys. Chem. B* **105**:4464-4470 (2001).
- [12] I. Szleifer et al, *Phys. Rev. Lett.* **60**:1966-1969 (1988); I. Szleifer et al, *J. Chem. Phys.* **92**:6800-6817 (1990).
- [13] V.S. Markin, *Biophys. J.* **36**: 1-19 (1981); W. Helfrich and M.M. Kozlov, *J. Phys. II France*, **4**:1427-1438 (1994).
- [14] A. Imparato, J.C. Shillcock and R. Lipowsky, *Eur. Phys. J. E* **11**:21-28 (2003).
- [15] R. Goetz and R. Lipowsky, *J. Chem. Phys.* **108**:7397-7409 (1998).
- [16] C. Leidy et al. *Biophys. J.* **80**:1819–1828 (2001); A.H. de Vries, A.E. Mark, S.J. Marrink *J. Phys. Chem. B* **108**:2454–2463 (2004); R. Faller and S.J. Marrink, *Langmuir* **20**:7686–7693 (2004); S. A. Pandit et al. *Biophys. J.* **87**:1092–1100 (2004).
- [17] R. Lipowsky and S. Grotehans, *Europhys. Lett.* **277**:599-604 (1993); and *Biophys. Chem.* **49**: 27-37 (1994).
- [18] A. Imparato, PhD thesis, University of Potsdam, Germany 2003.
- [19] F. David and S. Leibler, *J. Phys. France* **1**:959-976 (1991).
- [20] H. Engelhardt, H.P. Duwe and E. Sackmann, *J. Phys. (Paris) Lett.* **46**:395 (1985).
- [21] E.A. Evans, *Biophys. J.* **43**:27 (1983).
- [22] I. Bivas et al, *J. Phys. (Paris)* **48**:855 (1987).
- [23] J.M. di Meglio, M. Dvolaitzky, L. Leger, and C. Taupin *Phys. Rev. Lett.* **54**: 1686-1689 (1985)
- [24] C. R. Safinya et al, *Phys. Rev. Lett.* **57**: 2718-2721 (1986).
- [25] C. R. Safinya, E. B. Sirota, D. Roux, and G. S. Smith *Phys. Rev. Lett.* **62**: 1134-1137 (1989).
- [26] N. Lei and X. Lei, *Langmuir* **14**:2155-2159 (1998).